GEOLOGY | THE GEOLOGICAL SOCIETY OF AMERICA®

https://doi.org/10.1130/G47745.1

Manuscript received 4 February 2020
Revised manuscript received 26 July 2020
Manuscript accepted 27 July 2020

Reconstructing crustal thickness evolution from europium anomalies in detrital zircons

Ming Tang[1,2]*, Wei-Qiang Ji[3]*, Xu Chu[4], Anbin Wu[5] and Chen Chen[2,6]
[1]School of Earth and Space Sciences, Peking University, Beijing 100871, China
[2]Department of Earth, Environmental and Planetary Sciences, Rice University, Houston, Texas 77005, USA
[3]State Key Laboratory of Lithospheric Evolution, Institute of Geology and Geophysics, Chinese Academy of Sciences, P.O. Box 9825, Beijing 100029, China
[4]Department of Earth Sciences, University of Toronto, 22 Russell Street, Toronto, Ontario M5S 3B1, Canada
[5]College of Geoscience, China University of Petroleum, Beijing, China
[6]Key Laboratory of Mineralogy and Metallogeny, Guangzhou Institute of Geochemistry, Chinese Academy of Sciences, Guangzhou 510640, China

ABSTRACT

A new data compilation shows that in intermediate to felsic rocks, zircon Eu/Eu* [chondrite normalized Eu/$\sqrt{(\mathrm{Sm}\times\mathrm{Gd})}$] correlates with whole rock La/Yb, which has been be used to infer crustal thickness. The resultant positive correlation between zircon Eu/Eu* and crustal thickness can be explained by two processes favored during high-pressure differentiation: (1) supression of plagioclase and (2) endogenic oxidation of Eu^{2+} due to garnet fractionation. Here we calibrate a crustal thickness proxy based on Eu anomalies in zircons. The Eu/Eu*-in-zircon proxy makes it possible to reconstruct crustal thickness evolution in magmatic arcs and orogens using detrital zircons. To evaluate this new proxy, we analyzed detrital zircons separated from modern river sands in the Gangdese belt, southern Tibet. Our results reveal two episodes of crustal thickening (to 60–70 km) since the Cretaceous. The first thickening event occurred at 90–70 Ma, and the second at 50–30 Ma following Eurasia-India collision. These findings are temporally consistent with contractional deformation of sedimentary strata in southern Tibet.

INTRODUCTION

Crustal thickness profoundly influences a number of geologic processes including magmatic differentiation (Ducea, 2002; Ducea et al., 2015; Farner and Lee, 2017; Tang et al., 2018), ore formation (Kay, 2001; Lee and Tang, 2020), and erosion and weathering (Larsen et al., 2014). However, resolving the evolution of crustal thickness has been challenging. Because of erosion, weathering, and tectonic processes, the continental crust has been subject to constant destruction and overprinting after its formation, so the preserved continental crust may not reflect how thick it was when the crust was first generated.

Recent studies found that certain element ratios (e.g., Sr/Y and La/Yb) in intermediate to felsic rocks correlate with crustal thickness (Chapman et al., 2015; Profeta et al., 2015). As the crust thickens, the increased pressure of magmatic differentiation enhances amphibole and/or garnet fractionation relative to plagioclase. Amphibole and garnet fractionations deplete middle and heavy rare earth elements (REEs), respectively, relative to light REEs and Sr. The La/Yb and Sr/Y approaches extract differentiation pressure and thus crustal thickness from magmatic records, and their effectiveness has been demonstrated by a number of studies of Phanerozoic orogens (Chapman et al., 2015; Farner and Lee, 2017; Haschke et al., 2002). Despite their successful applications, these whole rock chemistry methods require extensive sampling over large areas in the field, and sample availability can be strongly biased by accessibility; for deep time, their applications are further limited by the increasingly significant issue of preservation of rock records.

Here we extend the arena of rock chemistry–based crustal thickness proxies by linking zircon Eu anomaly to whole rock La/Yb ratio. Zircon is ubiquitous in the continental crust and can survive most metamorphic, erosional, and weathering processes due to its refractory nature. Detrital zircons naturally sample large areas exposed to erosion and may fill gaps in Earth's history where rock records are missing (Balica et al., 2019; McKenzie et al., 2016, 2018; Zhu et al., 2020). We first calibrate the zircon crustal thickness proxy against the whole rock La/Yb proxy. Then, we evaluate the zircon proxy with a case study of the Gangdese belt, southern Tibet, where independent geologic constraints on crustal thickening and/or shortening exist.

*E-mails: mingtang@pku.edu.cn, jiweiqiang@mail.iggcas.ac.cn

RATIONALE

Europium anomaly [Eu/Eu*; chondrite normalized Eu/$\sqrt{(\mathrm{Sm}\times\mathrm{Gd})}$] in zircon is dictated by Eu/Eu* in the melt and Sm-Eu-Gd partitioning between zircon and melt. Unlike other REEs which are trivalent (except Ce), Eu exists as both Eu^{2+} and Eu^{3+} in most magmatic systems. Eu^{2+} is geochemically similar to Sr^{2+} and thus strongly partitions into plagioclase (Ren, 2004). Plagioclase fractionation causes Eu depletion relative to neighboring Sm and Gd in the residual melt. As a consequence, zircons crystallizing from the residual melt would have negative Eu anomalies, or Eu/Eu* <1 (Holder et al., 2020). Eu/Eu* in zircon is also sensitive to Eu^{2+}/Eu^{3+} in the melt because Eu^{2+} is significantly more incompatible than Eu^{3+} in zircon lattice, as inferred from Sr^{2+} partitioning in zircon (Thomas et al., 2002).

As the crust thickens, the intracrustal differentiation through anatexis or fractional crystallization takes place at higher pressures, which suppresses plagioclase (e.g., Green, 1982) and

CITATION: Tang, M., et al., 2020, Reconstructing crustal thickness evolution from europium anomalies in detrital zircons: Geology, v. 49, p. , https://doi.org/10.1130/G47745.1

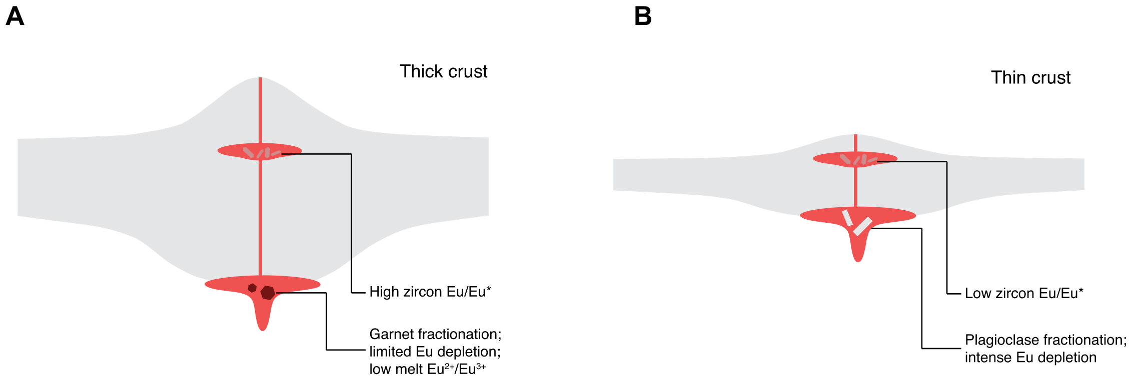

Figure 1. Cartoon (not to scale) showing influence of crustal thickness on Eu systematics in intracrustal differentiation. Crustal thickening destabilizes plagioclase and stabilizes garnet in deep crust, which reduces Eu depletion and oxidizes Eu in derivative melt. Eu/Eu*—chondrite normalized Eu/$\sqrt{(Sm \times Gd)}$.

thus prevents Eu depletion in the melt. In addition, intense crustal thickening stabilizes garnet, which preferentially sequesters Fe^{2+} over Fe^{3+} from the melt. The elevated $Fe^{3+}/\sum Fe$ (ferric Fe to total Fe ratio) in the melt would then oxidize multivalent trace elements such as Eu (Tang et al., 2018, 2019). Europium oxidation converts the less-compatible Eu^{2+} to more-compatible Eu^{3+}, which enhances Eu partitioning in zircon. The collective effect is that zircon Eu/Eu* increases with increasing crustal thickness (Fig. 1).

CALIBRATING THE EU/EU*-IN-ZIRCON CRUSTAL THICKNESS PROXY

We compiled 120 igneous samples with paired zircon–whole rock composition data. These samples are from 29 localities around the world. The whole rocks generally have intermediate to felsic compositions with SiO_2 contents of 55–75 wt%. We did not include more mafic samples because mafic rocks are not important sources of zircon; we also ignored high-silica samples (SiO_2 >75 wt%) because Eu systematics may be complicated by extreme differentiation (Fig. S3 in the Supplemental Material[1]). We divided our compiled samples into post-Archean and Archean groups. Post-Archean samples were further divided into I-type (igneous protoliths), S-type (sedimentary protoliths), A-type (shallow emplacement) granitoids based on the classification in the source literature. The Archean samples are represented by TTGs (tonalite-trondhjemite-granodiorite), which belong to I-type by definition.

I-type, including Archean TTGs, and A-type samples all fall on a positive correlation between zircon Eu/Eu* and whole rock $[La/Yb]_N$ (the subscript N denotes chondrite normalized) (Fig. 2A). This prominent relationship suggests that, on the first order, Eu/Eu* in zircon is controlled by the differentiation pressure which correlates with crustal thickness (McKenzie et al., 2018), despite the various complexities associated with global sample compilation. In particular, redox conditions seem to play a less-important role in determining Eu/Eu* in zircons from felsic magmas, or redox conditions of felsic magmas also correlate with differentiation pressure in most I- and A-type granitoids (Tang et al., 2018, 2019). S-type samples show no correlation between zircon Eu/Eu* and whole

[1]Supplemental Material. Methods, supplemental figures, and data. Please visit https://doi.org/10.1130/GEOL.S.12869660 to access the supplemental material, and contact editing@geosociety.org with any questions.

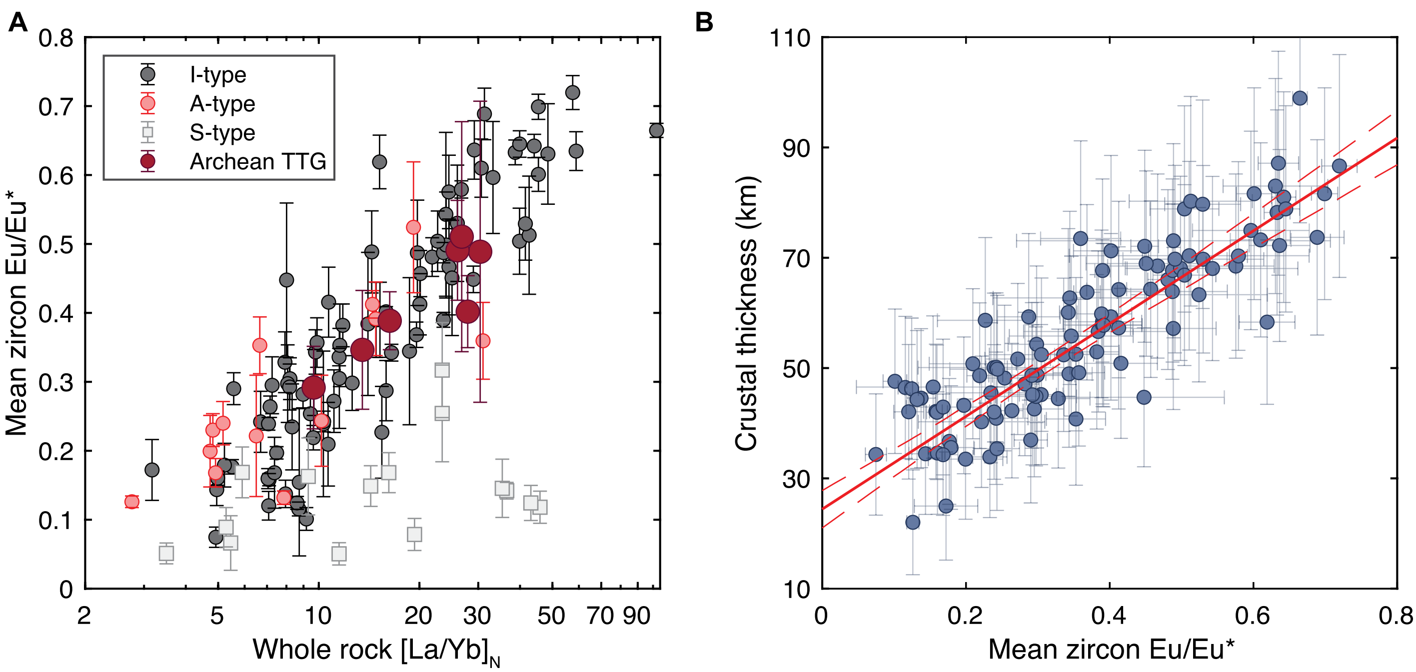

Figure 2. (A) Zircon Eu/Eu* [chondrite normalized Eu/$\sqrt{(Sm \times Gd)}$] versus whole rock $[La/Yb]_N$ (N—chondrite normalized). (B) Crustal thickness–zircon Eu/Eu* regression. Each data point represents mean of multiple analyses of zircons extracted from individual rock sample. Errors are two standard errors. Linear regression (mean and 95% confidence interval shown by the solid and dashed red lines, respectively) in B was obtained using post-Archean I-type samples, post-Archean A-type samples, and Archean tonalite-trondhjemite-granodiorite (TTG) samples. Errors of crustal thickness were derived from Profeta et al. (2015).

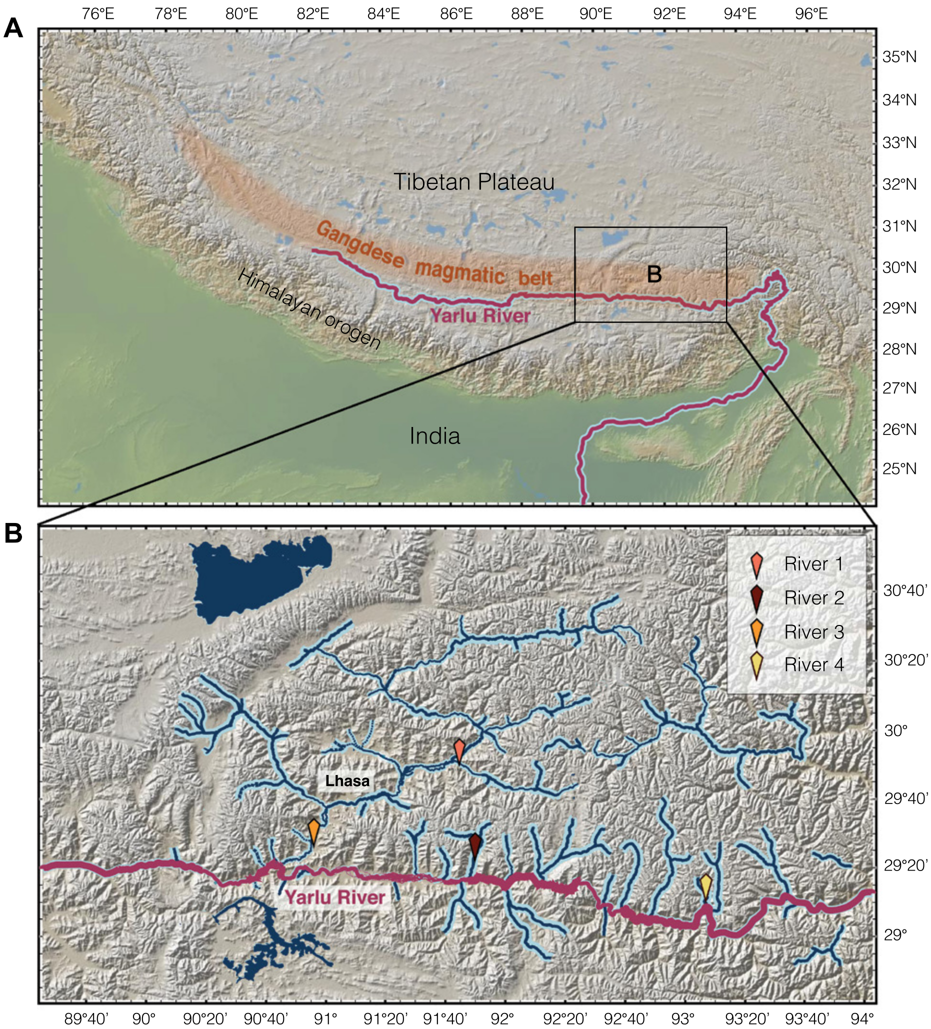

Figure 3. Maps showing river sand collecting sites and tributaries of the Yarlu River (Yarlung Tsangpo) in the sampling area, southern Tibet. All sand samples were collected in tributaries instead of the Yarlu River, which also receives detritus from the Himalayan orogen to the south. GeoMapApp software (http://www.geomapapp.org/) was used in making maps.

rock $[La/Yb]_N$ (Fig. 2A). The consistently low Eu/Eu* in these samples is likely inherent from the sedimentary protoliths derived from the Eu-depleted upper continental crust (Rudnick and Gao, 2014). Alternatively, the sedimentary protoliths of S-type granitoids may contain substantial amounts of reduced phases such as graphite and sulfides (Burnham and Berry, 2017; Chappell and White, 1992) that lead to highly reduced conditions and conversion of Eu^{3+} in the melt to less-compatible Eu^{2+}.

The positive correlation between zircon Eu/Eu* and whole rock $[La/Yb]_N$ in most intermediate to felsic samples affirms the feasibility of using zircon Eu/Eu* to reconstruct crustal thickness (McKenzie et al., 2018). Using modern arc samples, Profeta et al. (2015) derived an empirical relationship between whole rock $[La/Yb]_N$ and crustal thickness. Combining this relationship with the correlation between zircon Eu/Eu* and whole rock $[La/Yb]_N$ (Fig. 2B), we arrived at an empirical equation that calculates crustal thickness from zircon Eu/Eu* (Fig. 2B):

$$z = (84.2 \pm 9.2) \times \mathrm{Eu/Eu}^*_{\mathrm{zircon}} + (24.5 \pm 3.3), \quad (1)$$

where z is crustal thickness (in km). The uncertainties of the slope and intercept are two standard deviations. In this linear regression, we used all of our compiled samples except the S-type samples because their zircon Eu/Eu* does not correlate with whole rock $[La/Yb]_N$.

APPLICATION OF THE EU/EU*-IN-ZIRCON CRUSTAL THICKNESS PROXY IN SOUTHERN TIBET

Our new proxy makes it possible to reconstruct crustal thickness using detrital zircons. The Gangdese magmatic belt in southern Tibet provides an ideal case to evaluate this proxy. Southern Tibet transitioned from an Andean-type convergent margin in the Mesozoic to a collisional orogen in the Cenozoic (Allégre et al., 1984). The Gangdese belt has been magmatically active in the last ~200 m.y. (Chu et al., 2006), and the batholith is dominated by I-type granitic rocks at all ages (Ji et al., 2009).

We collected river sands from four modern rivers draining the eastern Gangdese batholith (Fig. 3). Detrital zircons were separated from these river sands and analyzed for simultaneous U-Pb ages and trace elements by laser ablation–inductively coupled plasma–mass spectrometry (LA-ICP-MS). We measured a total of 1639 detrital zircons. Detailed descriptions of the analytical methods and data are provided in the Supplemental Material. We removed analyses with Th/U <0.1 and/or La >1 ppm to eliminate metamorphic zircons and the data compromised by inclusions (Hoskin and Schaltegger, 2003). When calculating age-binned average crustal thickness, we removed analyses showing the highest 10% and lowest 10% Eu/Eu* within each 5 m.y. interval to reduce scatter. This screening procedure does not change the calculated crustal thickness pattern (Fig. S5).

Our reconstructed crustal thickness shows that the Gangdese belt started with a crustal thickness of ~40 km in the Early Cretaceous, then gradually thickened to ~60 km at ca. 80 Ma. The crust then thinned to ~50 km before it thickened again to ~70 km starting in the Eocene (Fig. 4A). Overall, the crustal thickness pattern reconstructed from detrital zircons mirrors that calculated using whole rock La/Yb, although some inconsistencies exist where the sample densities are low for both zircons and rocks (Fig. 4).

Opinions diverge when it comes to the crustal thickness in the Late Cretaceous. Both whole rock geochemistry and detrital zircon Eu/Eu* point to high-pressure origins for the Late Cretaceous granites in the Gangdese batholith. Ji et al. (2014) attributed the high La/Yb and Sr/Y ratios in the Late Cretaceous granites to intense crustal thickening, whereas Zhu et al. (2017) suggested these granites might have been generated by slab melting without crustal thickening. Zircon Eu/Eu*cannot distinguish between high-pressure intracrustal differentiation and slab melting, but the Late Cretaceous thickening scenario is more consistent with a number of regional geologic observations including sedimentary strata transitioning from marine limestone to clastic red beds followed by contractional deformation, north-south crustal shortening in the Lhasa terrane, and progressive burial of middle to lower crustal rocks in the Gangdese belt at that time (Burg et al., 1983; Kapp et al., 2007; Leier et al., 2007; Cao et al., 2020).

It is interesting to note that the crustal thickness decreased by ~10 km at the end of the Cretaceous (Fig. 4A). One possible explanation is that the lower crust was delaminated (Ji et al., 2014). Coupled magmatism and

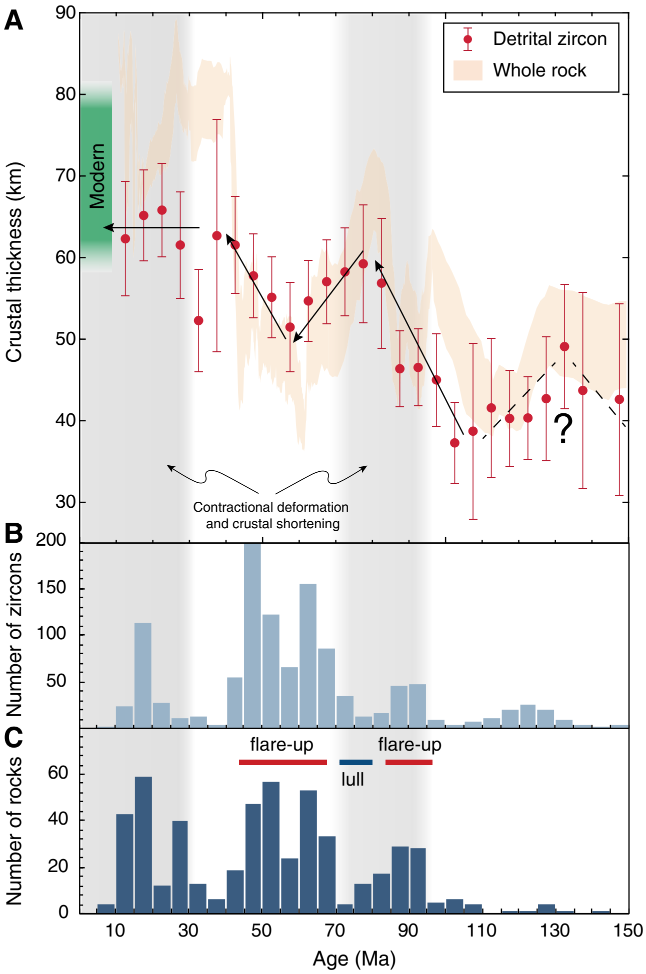

Figure 4. (A) Crustal thickness evolution of the Gangdese magmatic belt, southern Tibet, reconstructed from Eu/Eu* [chondrite normalized Eu/$\sqrt{(Sm \times Gd)}$] in detrital zircons (n = 1477). Data are plotted as binned averages for every 5 m.y. interval with two standard errors. Also shown here is crustal thickness calculated using the whole-rock La/Yb method (Profeta et al., 2015), plotted as running averages with two-standard-error intervals (orange band). Gangdese whole-rock La/Yb data are from Chapman and Kapp (2017). Timing of contractional deformation and crustal shortening in southern Tibet is from Kapp et al. (2007) and Leier et al. (2007). Black arrows and dashed lines illustrate the arbitrary trends of crustal thickening and thinning. (B) Age distribution of detrital zircons analyzed in this study. (C) Age distribution of Gangdese magmatic rocks compiled by Ji et al. (2014).

crustal shortening may have produced a thick layer of garnet-bearing cumulates (arclogites) in the lower Gangdese arc crust at ca. 70 Ma. These deep-arc cumulates are denser than the underlying peridotites and may eventually sink into the mantle. Alternatively, the Gangdese belt may have undergone a ~20 m.y. transient extension in response to slab rollback (Wang et al., 2015; Zhu et al., 2015). This transient extension may have triggered the magmatic flare-up at the Mesozoic-Cenozoic boundary (Fig. 4).

CAVEATS AND LIMITATIONS

Although the average zircon Eu/Eu* systematically increases with increasing whole rock La/Yb (Fig. 2A), significant scatter exists within individual samples (Fig. S2). A variety of factors may contribute to this scatter. For example, plagioclase co-crystallizing with zircon in the shallow magma chambers may deplete Eu in the melt and cause low Eu/Eu* in zircon. Assimilation of matured crustal materials may also affect Eu/Eu* in the melt and thus Eu/Eu* in zircon. Redox variation in melts changes Eu valence state and thus Eu partitioning in zircon (Holder et al., 2020). Given these complexities, the robustness of the calculated crustal thickness can be sensitive to the number of zircon analyses. We suggest that a histogram of zircon age distribution (Fig. 4B) should be provided side by side with the calculated crustal thickness evolution. We further suggest that interpretations of crustal thickness changes should be made based on evolution patterns instead of isolated anomalies.

S-type granitoids may also complicate the use of detrital zircons to reconstruct crustal thickness because Eu/Eu* in S-type granitoid zircons does not reflect crustal thickness (Fig. 2A). The Gangdese belt presents a simple case where S-type granitoids are scarce. But in other orogens, S-type granitoids may be a more important source of detrital zircons. Zircons from S-type granitoids can be identified by their phosphorus contents (Burnham and Berry, 2017; Zhu et al., 2020), and should be filtered out before applying the zircon crustal thickness proxy in places with complex lithologies.

Finally, our proxy may not apply to zircons crystallized from high-silica melts (SiO_2 >75 wt%) due to complex Eu/Eu* systematics and an overstretch of the whole rock La/Yb proxy in these extremely differentiated samples. However, we find that igneous rocks with SiO_2 >75 wt% are minor (~5% in magmatic arcs; Fig. S3) and are probably dominated by S-type granitoids whose zircons can be filtered out by their phosphorus contents.

CONCLUSIONS AND OUTLOOK

Zircon Eu/Eu* positively correlates with whole rock $[La/Yb]_N$ in most intermediate to felsic igneous samples. This correlation allows one to use zircon Eu/Eu* to estimate the La/Yb of the parent magmas, which in turn gives crustal thickness. Application of the Eu/Eu*-in-zircon crustal thickness proxy to Gangdese detrital zircons reveals at least two episodes of crustal thickening in the last 150 m.y. that are in phase with field observations in the Gangdese magmatic belt.

Our Eu/Eu*-in-zircon crustal thickness proxy is not to replace whole rock trace element proxies, but the zircon approach opens the window for extracting crustal thickness information from the extensive detrital zircon archive and may provide a continuous record of crustal thickness evolution. By integrating age, geochemistry, and crustal thickness, the detrital zircon archive can now be used to reconstruct coupled tectonic and magmatic history in continental evolution.

ACKNOWLEDGMENTS

This work is supported by the National Natural Science Foundation of China (grant 41888101) and the China State Key Laboratory of Lithospheric Evolution (grant SKL-Z201706). Tang is grateful for the support by a U.S. National Science Foundation grant (EAR-1850832) and a Beijing "Double-First Class" initiative grant (7101302526). We thank Ryan McKenzie, Michael Farner, and two anonymous reviewers for their comments and editor James Schmitt for efficient handling. We also thank Cin-Ty A. Lee, Bo Wan, Wenrong Cao, and Fuyuan Wu for insightful discussions.

REFERENCES CITED

Allégre, C.J., et al., 1984, Structure and evolution of the Himalaya–Tibet orogenic belt: Nature, v. 307, p. 17, https://doi.org/10.1038/307017a0.

Balica, C., et al., 2019, A zircon petrochronologic view on granitoids and continental evolution: Earth and Planetary Science Letters, v. 531, 116005, https://doi.org/10.1016/j.epsl.2019.116005.

Burg, J.-P., Proust, F., Tapponnier, P., and Ming, C.G., 1983, Deformation phases and tectonic evolution of the Lhasa block (southern Tibet, China): Eclogae Geologicae Helvetiae, v. 76, p. 643–665.

Burnham, A.D., and Berry, A.J., 2017, Formation of Hadean granites by melting of igneous crust: Nature Geoscience, v. 10, p. 457–461, https://doi.org/10.1038/ngeo2942.

Cao, W., Yang, J., Zuza, A.V., Ji, W.-Q., Ma, X.-X., Chu, X., and Burgess, Q.P., 2020, Crustal tilting and differential exhumation of Gangdese Batholith in southern Tibet revealed by bedrock pressures: Earth and Planetary Science Letters, v. 543, p. 116347.

Chapman, J.B., and Kapp, P., 2017, Tibetan magmatism database: Geochemistry Geophysics Geosystems, v. 18, p. 4229–4234, https://doi.org/10.1002/2017GC007217.

Chapman, J.B., Ducea, M.N., DeCelles, P.G., and Profeta, L., 2015, Tracking changes in crustal thickness during orogenic evolution with Sr/Y:

An example from the North American Cordillera: Geology, v. 43, p. 919–922, https://doi.org/10.1130/G36996.1.

Chappell, B.W., and White, A.J.R., 1992, I- and S-type granites in the Lachlan Fold Belt: Earth and Environmental Science Transactions of the Royal Society of Edinburgh, v. 83, p. 1–26, https://doi.org/10.1017/S0263593300007720.

Chu, M.-F., Chung, S.-L., Song, B., Liu, D., O'Reilly, S.Y., Pearson, N.J., Ji, J., and Wen, D.-J., 2006, Zircon U-Pb and Hf isotope constraints on the Mesozoic tectonics and crustal evolution of southern Tibet: Geology, v. 34, p. 745–748, https://doi.org/10.1130/G22725.1.

Ducea, M.N., 2002, Constraints on the bulk composition and root foundering rates of continental arcs: A California arc perspective: Journal of Geophysical Research, v. 107, 2304, https://doi.org/10.1029/2001JB000643.

Ducea, M.N., Saleeby, J.B., and Bergantz, G., 2015, The architecture, chemistry, and evolution of continental magmatic arcs: Annual Review of Earth and Planetary Sciences, v. 43, p. 299–331, https://doi.org/10.1146/annurev-earth-060614-105049.

Farner, M.J., and Lee, C.-T.A., 2017, Effects of crustal thickness on magmatic differentiation in subduction zone volcanism: A global study: Earth and Planetary Science Letters, v. 470, p. 96–107, https://doi.org/10.1016/j.epsl.2017.04.025.

Green, T.H., 1982, Anatexis of mafic crust and high pressure crystallization of andesite, *in* Thorpe, R.S., ed., Andesites: Orogenic Andesites and Related Rocks: New York, John Wiley & Sons, p. 465–487.

Haschke, M.R., Scheuber, E., Günther, A., and Reutter, K.-J., 2002, Evolutionary cycles during the Andean orogeny: Repeated slab breakoff and flat subduction?: Terra Nova, v. 14, p. 49–55, https://doi.org/10.1046/j.1365-3121.2002.00387.x.

Holder, R.M., Yakymchuk, C., and Viete, D.R., 2020, Accessory mineral Eu anomalies in suprasolidus rocks: Beyond feldspar: Geochemistry Geophysics Geosystems, e2020GC009052, https://doi.org/10.1029/2020GC009052 (in press).

Hoskin, P.W.O., and Schaltegger, U., 2003, The composition of zircon and igneous and metamorphic petrogenesis: Reviews in Mineralogy and Geochemistry, v. 53, p. 27–62, https://doi.org/10.2113/0530027.

Ji, W.-Q, Wu, F.-Y., Liu, C.-Z., and Chung, S.-L., 2009, Geochronology and petrogenesis of granitic rocks in Gangdese batholith, southern Tibet: Science in China: Series D, Earth Sciences, v. 52, p. 1240–1261, https://doi.org/10.1007/s11430-009-0131-y.

Ji, W.-Q., Wu, F.-Y., Chung, S.-L., and Liu, C.-Z., 2014, The Gangdese magmatic constraints on a latest Cretaceous lithospheric delamination of the Lhasa terrane, southern Tibet: Lithos, v. 210, p. 168–180, https://doi.org/10.1016/j.lithos.2014.10.001.

Kapp, P., DeCelles, P.G., Gehrels, G.E., Heizler, M., and Ding, L., 2007, Geological records of the Lhasa-Qiangtang and Indo-Asian collisions in the Nima area of central Tibet: Geological Society of America Bulletin, v. 119, p. 917–933, https://doi.org/10.1130/B26033.1.

Kay, S.M., 2001, Central Andean ore deposits linked to evolving shallow subduction systems and thickening crust: GSA Today, v. 11, no. 3, p. 4–9, https://doi.org/10.1130/1052-5173(2001)011<0004:CAODLT>2.0.CO;2.

Larsen, I.J., Montgomery, D.R., and Greenberg, H.M., 2014, The contribution of mountains to global denudation: Geology, v. 42, p. 527–530, https://doi.org/10.1130/G35136.1.

Lee, C.-T.A., and Tang, M., 2020, How to make porphyry copper deposits: Earth and Planetary Science Letters, v. 529, 115868, https://doi.org/10.1016/j.epsl.2019.115868.

Leier, A.L., DeCelles, P.G., Kapp, P., and Ding, L., 2007, The Takena Formation of the Lhasa terrane, southern Tibet: The record of a Late Cretaceous retroarc foreland basin: Geological Society of America Bulletin, v. 119, p. 31–48, https://doi.org/10.1130/B25974.1.

McKenzie, N.R., Horton, B.K., Loomis, S.E., Stockli, D.F., Planavsky, N.J., and Lee, C.-T.A., 2016, Continental arc volcanism as the principal driver of icehouse-greenhouse variability: Science, v. 352, p. 444–447, https://doi.org/10.1126/science.aad5787.

McKenzie, N.R., Smye, A.J., Hegde, V.S., and Stockli, D.F., 2018, Continental growth histories revealed by detrital zircon trace elements: A case study from India: Geology, v. 46, p. 275–278, https://doi.org/10.1130/G39973.1.

Profeta, L., Ducea, M.N., Chapman, J.B., Paterson, S.R., Gonzales, S.M.H., Kirsch, M., Petrescu, L., and DeCelles, P.G., 2015, Quantifying crustal thickness over time in magmatic arcs: Scientific Reports, v. 5, 17786, https://doi.org/10.1038/srep17786.

Ren, M., 2004, Partitioning of Sr, Ba, Rb, Y, and LREE between alkali feldspar and peraluminous silicic magma: American Mineralogist, v. 89, p. 1290–1303, https://doi.org/10.2138/am-2004-8-918.

Rudnick, R.L., and Gao, S., 2014, Composition of the continental crust, *in* Rudnick, R.L., ed., Treatise on Geochemistry (second edition), Volume 4: The Crust: Oxford, UK, Elsevier, p. 1–51, https://doi.org/10.1016/B978-0-08-095975-7.00301-6.

Tang, M., Erdman, M., Eldridge, G., and Lee, C.-T.A., 2018, The redox "filter" beneath magmatic orogens and the formation of continental crust: Science Advances, v. 4, eaar4444, https://doi.org/10.1126/sciadv.aar4444.

Tang, M., Lee, C.-T.A., Costin, G., and Höfer, H.E., 2019, Recycling reduced iron at the base of magmatic orogens: Earth and Planetary Science Letters, v. 528, 115827, https://doi.org/10.1016/j.epsl.2019.115827.

Thomas, J.B., Bodnar, R.J., Shimizu, N., and Sinha, A.K., 2002, Determination of zircon/melt trace element partition coefficients from SIMS analysis of melt inclusions in zircon: Geochimica et Cosmochimica Acta, v. 66, p. 2887–2901, https://doi.org/10.1016/S0016-7037(02)00881-5.

Wang, R., Richards, J.P., Hou, Z.-q., An, F., and Creaser, R.A., 2015, Zircon U-Pb age and Sr-Nd-Hf-O isotope geochemistry of the Paleocene–Eocene igneous rocks in western Gangdese: Evidence for the timing of Neo-Tethyan slab breakoff: Lithos, v. 224, p. 179–194, https://doi.org/10.1016/j.lithos.2015.03.003.

Zhu, D.-C., Wang, Q., Zhao, Z.-D., Chung, S.-L., Cawood, P.A., Niu, Y., Liu, S.-A., Wu, F.-Y., and Mo, X.-X., 2015, Magmatic record of India-Asia collision: Scientific Reports, v. 5, 14289, https://doi.org/10.1038/srep14289.

Zhu, D.-C., Wang, Q., Cawood, P.A., Zhao, Z.-D., and Mo, X.-X., 2017, Raising the Gangdese Mountains in southern Tibet: Journal of Geophysical Research: Solid Earth, v. 122, p. 214–223, https://doi.org/10.1002/2016JB013508.

Zhu, Z., Campbell, I.H., Allen, C.M., and Burnham, A.D., 2020, S-type granites: Their origin and distribution through time as determined from detrital zircons: Earth and Planetary Science Letters, v. 536, 116140, https://doi.org/10.1016/j.epsl.2020.116140.

Printed in USA